processes

MDPI

Article

A Two-Stage Stochastic Programming Approach for the Design of Renewable Ammonia Supply Chain Networks

Ilias Mitrai, Matthew J. Palys and Prodromos Daoutidis *

Department of Chemical Engineering and Materials Science, University of Minnesota, Minneapolis, MN 55455, USA; mitra047@umn.edu (I.M.); palys003@umn.edu (M.J.P.)
* Correspondence: daout001@umn.edu

Abstract: This work considers the incorporation of renewable ammonia manufacturing sites into existing ammonia supply chain networks while accounting for ammonia price uncertainty from existing producers. We propose a two-stage stochastic programming approach to determine the optimal investment decisions such that the ammonia demand is satisfied and the net present cost is minimized. We apply the proposed approach to a case study considering deploying in-state renewable ammonia manufacturing in Minnesota's supply chain network. We find that accounting for price uncertainty leads to supply chains with more ammonia demand met via renewable production and thus lower costs from importing ammonia from existing producers. These results show that the in-state renewable production of ammonia can act as a hedge against the volatility of the conventional ammonia market.

Keywords: supply chain optimization; capacity expansion; stochastic optimization; green ammonia

Citation: Mitrai, I.; Palys, M.J.; Daoutidis, P. A Two-Stage Stochastic Programming Approach for the Design of Renewable Ammonia Supply Chain Networks. *Processes* **2024**, *12*, 325. https://doi.org/10.3390/pr12020325

Academic Editor: Michael C. Georgiadis and Nikolaos A. Diangelakis

Received: 16 January 2024
Revised: 30 January 2024
Accepted: 31 January 2024
Published: 2 February 2024

1. Introduction

Ammonia is the backbone of modern agriculture since it is the basic ingredient of fertilizers. Traditionally, ammonia has been produced using the Haber–Bosch process, where hydrogen obtained from fossil fuels reacts with nitrogen at high temperature and pressure [1]. This manufacturing paradigm is based on high-capacity facilities, in the order of 10^6 metric tons per year (mt/y), to take advantage of economies of scale [2]. Ammonia is then distributed from these few production sites to the final customers via an expansive network of ships, rails, and trucks, which form national and even global supply chain networks [3].

Currently, significant efforts are being devoted to industrial decarbonization and sustainability [4]. A sustainable ammonia supply chain network requires a reduction in carbon emissions related to both production and distribution [5–7]. A low-carbon or "green" ammonia production paradigm has recently been the subject of extensive research and development as an alternative to the existing one [8]. In the green ammonia paradigm, the production carbon intensity is reduced using renewable resources, such as wind and solar, to produce hydrogen via electrolysis and nitrogen via air separation. If these resources are spatially distributed, there is also an opportunity to reduce the transportation carbon intensity, as ammonia can be produced closer to where it is ultimately consumed [9].

The Midwest region of the United States consumes the most nitrogen fertilizer in the country while being home to abundant wind energy resources [10]. This creates an opportunity to reduce the carbon intensity of ammonia supply chain networks from both production and transportation perspectives by manufacturing ammonia locally using this wind energy. Such local production can also offer fertilizer price stability. Renewable energy is the dominant operating cost in manufacturing renewable ammonia [11,12]. The price of this energy can be made relatively stable if obtained from multi-year power purchase agreements (PPAs) or through co-ownership of the renewable energy generation and

ammonia production facilities. In contrast, ammonia is currently traded on a global market and its price is highly volatile due to a number of factors such as natural gas prices, food prices, and global conflicts (see Figure 1) [13,14]. Realizing the full transformative potential of this local renewable ammonia paradigm requires the optimal transition away from current fossil-based ammonia supply chain networks.

This transition will occur over multiple years due to the investment required and the operational value of the existing conventional ammonia production and transportation assets. The problem of identifying the optimal investments over a fixed time horizon is known as the capacity expansion problem [15]. Recently, we proposed a multi-period deterministic capacity expansion model that considers the optimal transition of conventional ammonia supply chain networks to renewable ones [16]. In that work, we sought to find the optimal investment decisions regarding installation year, location, and capacity such that the net present cost is minimized while the ammonia fertilizer demand is satisfied.

In this work, we consider the effect of uncertainty on the transition of existing ammonia supply chain networks. In general, two types of uncertainties can affect supply chain networks. The first, called exogenous [17,18], refers to uncertainties from external factors, such as changes in demand or price. The second type, called endogenous, refers to decision-dependent uncertainties, such as changes in the cost of different technologies due to wider adoption [19,20]. We hereby focus on exogenous uncertainty. Stochastic optimization, specifically two-stage formulations, has been widely used for the design of supply chain networks in different industries, for example, biodiesel production from wastewater treatment byproducts [21], waste to bioethanol [22], ethanol [23], and coal to liquids [24]. Regarding ammonia supply chain networks, the primary sources of uncertainty are the ammonia demand and the market price of ammonia from existing producers. While ammonia demand can be predicted from the total estimated crop acreage requiring fertilizer, the price is more volatile as shown in Figure 1.

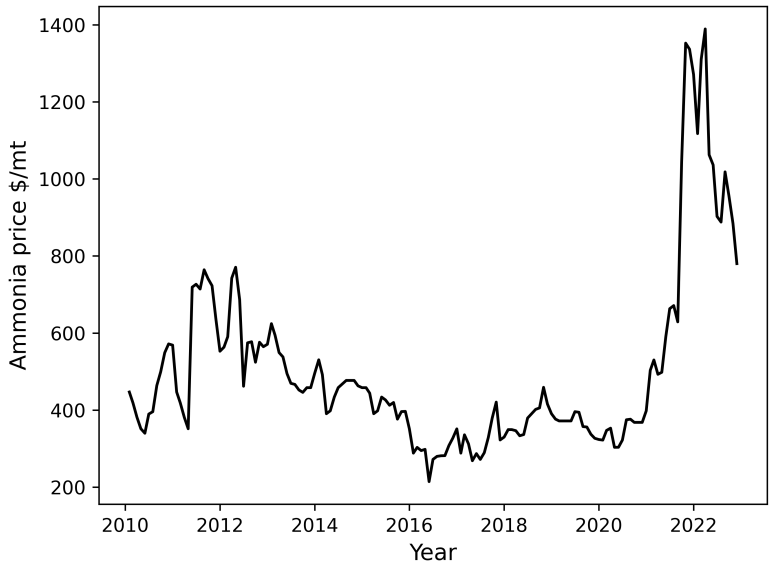

Figure 1. U.S. Gulf Coast ammonia price from 2010 to 2022 [25].

We propose a two-stage stochastic programming approach, where the uncertainty in price is considered in the form of scenarios [17,26]. The first-stage decisions are the location, capacity, and installation year for new renewable ammonia production facilities. The first-stage decisions are optimized once for a given optimization model instance. The second-stage decisions are the quantities of ammonia transported from the installed renewable sites and existing conventional producers to the customers and distribution centers. The second-stage decisions are optimized for different ammonia price scenarios. The resulting problem is a Mixed-Integer Linear Programming (MILP) problem. We consider a case study on Minnesota's ammonia supply chain network over a transition

horizon from 2024 to 2032. The results show that accounting for price uncertainty leads to a reduction in the amount of ammonia purchased over the planning horizon. Specifically, we find that higher renewable ammonia manufacturing capacity is installed in the stochastic case compared to the deterministic case. We also consider the transition to a supply chain that is constrained to be fully renewable by 2032. In this case, considering conventional ammonia price uncertainty results in earlier investments in renewable ammonia manufacturing compared to the deterministic case, leading to a reduction in the amount of ammonia purchased over the entire horizon. Simulation of the supply chain network designs obtained in both cases reveals that for high ammonia prices, the design obtained using the stochastic optimization model leads to lower net present cost. These results show that in-state ammonia manufacturing using renewable energy can act as a hedge against the volatility of the ammonia market price. Additionally, the supply chain designs obtained from stochastic optimization lead to lower average ammonia purchasing costs to the benefit of farmers.

The rest of the paper is organized as follows: In Section 2, we present the two-stage stochastic optimization model; in Section 3, we present the case study and the scenario generation procedure; and in Section 4, we present and discuss the results of the case study.

2. Two-Stage Stochastic Optimization Problem

We assume an existing ammonia supply chain network with C customers, D distribution centers, and P conventional ammonia producers. We define set $\mathcal{C} = \{1, \ldots, C\}$ as the set of customers, $\mathcal{D} = \{1, \ldots, D\}$ as the set of distribution centers, and $\mathcal{P} = \{1, \ldots, P\}$ as the set of existing conventional producers. Given this initial supply chain network and a set of candidate renewable ammonia production sites $\mathcal{R} = \{1, \ldots, R\}$, we seek to identify the optimal investment decisions over a planning horizon of N_t years ($\mathcal{K} = \{1, \ldots, N_t\}$). The model specifically optimizes the installation year, location, and capacity of new renewable production toward minimizing the net present cost of meeting the ammonia demand δ_{ck} for each customer in each year. We define a binary variable z_{rk} which is equal to one if renewable site r is installed at time period k and zero otherwise. We also define variable x_{rk} as the production capacity at site r installed at time period k. The first set of constraints defines the minimum and maximum capacity that can be installed at a candidate location r:

$$x_{rk} \leq \bar{x}^U z_{rk} \quad \forall r \in \mathcal{R}, k \in \mathcal{K} \tag{1}$$

$$x_{rk} \geq \bar{x}^L z_{rk} \quad \forall r \in \mathcal{R}, k \in \mathcal{K}, \tag{2}$$

where $\bar{x}^U = 1000$ mt/y and $\bar{x}^L = 50$ mt/y are the upper and lower bounds on the capacity that can be installed. These bounds are related to the relevant commercial availability range of the different technologies required to produce renewable ammonia (e.g., electrolysis, air separation, Haber-Bosch synthesis). The renewable ammonia production facilities obtain hydrogen via wind-powered electrolysis. Each candidate location r thus has specific maximum capacities of new renewable production enforced by the following constraints:

$$\sum_{k'=1}^{k} x_{rk'} \omega_{rk'} \leq \Omega_r \quad \forall r \in \mathcal{R}, k \in \mathcal{K} \tag{3}$$

$$\sum_{r \in \mathcal{R}} x_{rk} \xi_{rk} \leq \Xi_{rk} \quad \forall k \in \mathcal{K}, \tag{4}$$

where Ω_r is the wind capacity at site r, ω_{rk} is a conversion factor that links ammonia production with wind generation, Ξ_{rk} is the electrolysis capacity at location r and time period k, and ξ_{rk} is a conversion factor between mt/y of ammonia production and MW of electrolysis. These parameters depend on the installation year since electrolysis is expected to get more efficient over the years. The constraints in Equations (1)–(4) pertain to the first-stage decisions of the problem.

The second-stage decisions consider the flow of ammonia across the supply chain network for different conventional ammonia prices (scenarios). We define variable y_{pdks} as the amount of ammonia purchased from conventional producer p and shipped to distribution center d at time period k in scenario s, variable y_{dcks} as the amount of ammonia shipped from distribution center d to customer c at time period k in scenario s, and variable y_{rcks} as the amount of ammonia shipped from renewable site r to customer c at time period k in scenario s. The flow constraints in the supply chain network are:

$$\sum_{r\in\mathcal{R}} y_{rcks} + \sum_{d\in\mathcal{D}} y_{dcks} \geq \delta_{ck} \quad \forall s \in \mathcal{S}, c \in \mathcal{C}, k \in \mathcal{K} \tag{5}$$

$$\sum_{p\in\mathcal{P}} y_{pdks} \geq \sum_{c\in\mathcal{C}} y_{dcks} \quad \forall s \in \mathcal{S}, d \in \mathcal{D}, k \in \mathcal{K} \tag{6}$$

$$\sum_{d\in\mathcal{D}} y_{pdks} \leq \Lambda_p \quad \forall s \in \mathcal{S}, p \in \mathcal{P}, k \in \mathcal{K} \tag{7}$$

$$\sum_{c\in\mathcal{C}} y_{rcks} \leq \sum_{k'=1}^{k-\omega} x_{rk'} \quad \forall s \in \mathcal{S}, r \in \mathcal{R}, k \in \mathcal{K}. \tag{8}$$

The constraint in Equation (5) guarantees that the demand of customer c at time period k, δ_{ck}, is satisfied by ammonia purchased from conventional resources and transported from the distribution centers and by ammonia produced and transported from the installed renewable sites. Equation (6) guarantees that for each distribution center, the amount of ammonia received from the conventional producers is greater than or equal to the amount of ammonia shipped to the customers. The constraint in Equation (7) limits the maximum amount of ammonia purchased from conventional producer p at each time period and scenario s, with Λ_p being the maximum amount that can be purchased. Finally, Equation (8) sets the upper bound of the amount of ammonia shipped from a renewable site r to all the customers by the installed capacity while accounting for the construction time of ω years.

The objective function is the net present cost of the supply chain expansion over the entire planning horizon and comprises two terms. The first term accounts for the cost of installing and operating a new renewable ammonia production site. The capital cost CAP_k is modeled as a piece-wise affine function of the capacity, with slope σ_{rk} and intercept γ_{rk}, to capture the effect of economies of scales. These parameters vary with time for each candidate renewable site r to account for the renewable potential and expected technology cost reductions. The capital cost is scaled with the plant lifetime θ, which is equal to 10.23. We assume that the operating cost (OP_k) scales linearly with the capacity, with proportionality constant ζ_{rk}. The operating cost remains constant after installation and varies for the different renewable sites r to capture the effects described above. The equations that describe these costs for a given time period k are equal to

$$\begin{aligned} CAP_k &= \frac{1}{\theta} \sum_{r\in\mathcal{R}} \sum_{k'=1}^{k} x_{rk'}\sigma_{rk'} + z_{rk'}\gamma_{rk'} \\ OP_k &= \sum_{r\in\mathcal{R}} \sum_{k'=1}^{k} x_{rk'}\zeta_{rk'}. \end{aligned} \tag{9}$$

The second term in the objective function accounts for the purchase and distribution cost of ammonia for the different scenarios. We define PC_{ks} as the purchasing cost of ammonia from conventional resources for time period k and scenario s, DR_{ks} as the distribution cost of renewable ammonia at time period k and scenario s, TC_{ks} as the cost of transporting ammonia from conventional producers to distribution centers for period k and scenario s,

and DC_{ks} as the transportation cost from distribution centers to customers for period k and scenario s. The costs are defined as follows:

$$\begin{aligned} DR_{ks} &= \sum_{r\in\mathcal{R}}\sum_{c\in\mathcal{C}} y_{rcks}\tau_{rc} \quad \forall k \in \mathcal{K}, s \in \mathcal{S} \\ PC_{ks} &= \sum_{p\in\mathcal{P}}\sum_{d\in\mathcal{D}} y_{pdks}\alpha_{ps} \quad \forall k \in \mathcal{K}, s \in \mathcal{S} \\ TC_{ks} &= \sum_{p\in\mathcal{P}}\sum_{d\in\mathcal{D}} y_{pdks}\tau_{pd} \quad \forall k \in \mathcal{K}, s \in \mathcal{S} \\ DC_{ks} &= \sum_{d\in\mathcal{D}}\sum_{c\in\mathcal{C}} y_{dcks}\tau_{dc} \quad \forall k \in \mathcal{K}, s \in \mathcal{S}, \end{aligned} \tag{10}$$

where α_{ps} is the conventional ammonia cost from producer p and scenario s, τ_{rc} is the unit transportation cost from renewable site r to customer c, τ_{pd} is the unit transportation cost from conventional producer p to distribution center d, and τ_{dc} is the unit transportation cost from distribution center d to customer c.

Overall, the two-stage optimization problem is

$$\begin{aligned} \underset{\substack{x_{rk},z_{rk},y_{rcks}\\ y_{pdks},y_{dcks}}}{\text{minimize}} \quad & \sum_{k\in\mathcal{K}} \phi_k(CAP_k + OPk) + \sum_{s\in\mathcal{S}} \pi_s \left(\sum_{k\in\mathcal{K}} \phi_k(DR_{ks} + PC_{ks} + TC_{ks} + DC_{ks}) \right) \\ \text{subject to} \quad & \text{Equations } (1) - (8), \\ & x_{rk} \geq 0, z_{rk} \in \{0,1\}, y_{rcks} \geq 0, y_{pdks} \geq 0, y_{dcks} \geq 0, \end{aligned} \tag{11}$$

where ϕ_k is the discounted value of cost contributions at time period k and π_s is the probability of scenario s.

3. Case Study

3.1. Case Study Description

We consider a case study on Minnesota's ammonia supply chain network. For a detailed description, we refer the reader to [16]. We consider a planning horizon of nine years ($N_t = 9, |\mathcal{K}| = 9$) between 2024 and 2032. We also consider an 8.5% discount rate to account for weight cash flows in different years. The number of counties, i.e., customers, in Minnesota is 82 ($C = |\mathcal{C}| = 82$). The total ammonia demand for all counties for 2024 is 795,000 mt, and a 0.5% per year increase is assumed until the end of the horizon. Conventionally produced ammonia can be purchased from ten producers ($P = |\mathcal{P}| = 10$) which are located outside of Minnesota. This ammonia is routed to the counties via three distribution centers ($D = |\mathcal{D}| = 3$) located in Minnesota. Conventional producers located further from Minnesota have higher associated transportation costs. Producer-to-distribution transportation costs vary from 59 USD/mt to 141 USD/mt and distribution center-to-county costs range from 1 USD/mt to 36 USD/mt. The average price of conventional ammonia from 2010 to 2022 was 500 USD/mt.

We consider 26 candidate locations for new renewable ammonia production ($R = |\mathcal{R}| = 26$). The optimized capital cost, operating cost, and optimal nameplate capacity of wind generation, electrolysis, and ammonia synthesis capacity for a given ammonia production scale, location, and installation year are obtained from our previous work [16]. The capital cost of a new renewable ammonia facility is incurred two years ($\omega = 2$) before production starts to account for the construction time. The ammonia produced at renewable sites is transported directly to the counties with transportation costs ranging from 1 USD/mt to USD 47 USD/mt. The operating cost of a site includes renewable energy from PPAs with wind generation entities assumed to be co-located with the renewable ammonia facilities. Hydrogen production tax credits (PICs) [27] contained in the U.S. federal government Inflation Reduction Act are included in the operating cost as a negative quantity. These credits provide 3 USD/kg for the first ten years of hydrogen production. We assume that the capital and operating costs monotonically decrease over

time due to projected cost reductions and performance improvement in the constituent technologies, e.g., electrolysis. The decrease occurs in three-year periods with identical capital and operating cost for facilities installed in 2024 to 2027, 2027 through 2029, and 2030 through 2032. The capacity of each new renewable facility is constrained by a maximum wind generation capacity of 250 MW (Equation (3)) and the total installed capacity of new renewable ammonia production in each year is constrained by the electrolysis availability (Equation (4)), which increases from 250 MW in 2024 to 850 MW in 2032.

3.2. Generation of Scenarios

In this section, we consider the generation of the scenarios for the two-stage stochastic optimization problem. The price of ammonia in each scenario and the probability of that scenario are inputs to the stochastic programming problem. In this work, we use the distribution matching approach [28] for generating the scenario tree. In this approach, given the historical data regarding the realization of the uncertain parameters, the goal is to generate a scenario tree whose statistical properties are close to the properties of the distribution computed from the data. We define as $\mathcal{F} = \{\gamma_i\}_{i=1}^{N_\gamma}$ the set of moments that we want to match (N_γ is the number of moments). In the context of our work, we seek to find the ammonia price α_{ps} and probability π_s of each scenario such that the average (γ_1), variance (γ_2), skewness (γ_3), kurtosis (γ_4), and empirical cumulative distribution function of the scenario tree are as close as possible to those of the data. We define Γ_i as the value of moment i computed from the data and G as the approximation of the Cumulative Distribution Function (CDF) of the data. We assume that the ammonia price is the same for all conventional producers, so we use the notation α_s to denote the price at scenario s. The values of the ammonia price for each scenario and the associated probability are obtained from the solution of the following optimization problem:

$$\begin{aligned}
\underset{\pi_s, \alpha_s, \gamma_i, e_s}{\text{minimize}} \quad & \sum_{i=1}^{N_\gamma} w_i(\gamma_i - \Gamma_i)^2 + \sum_{s=1}^{N_s} e_s^2 \\
\text{subject to} \quad & \sum_{s\in\mathcal{S}} \pi_s = 1, \\
& \gamma_1 = \sum_{s\in\mathcal{S}} a_s \pi_s, \\
& \gamma_i = \sum_{s\in\mathcal{S}} (a_s - \gamma_1)^i \pi_s \;\; \forall i \geq 2, \ldots, N_\gamma, \\
& G(a_s) - \sum_{s'=1}^{s} \pi_{s'} = e_s \;\; \forall s \in \mathcal{S}, \\
& \alpha_s \leq \alpha_{s+1} \;\; \forall s \in \mathcal{S} \setminus \{N_s\}, \\
& \pi_s \in [0,1], \gamma_i \in [\gamma_i^{LB}, \gamma_i^{UB}], e_s \in R
\end{aligned} \tag{12}$$

where w_i is the weight for the moment i. We set $w_1 = 1/\Gamma_1^2$, $w_2 = 1/\Gamma_2^2$, $w_3 = 1/\Gamma_3$, $w_4 = 1/\Gamma_4$. The objective function has two terms. The first is a weighted summation of the squared error between the moments of the scenario tree and the moments from the data, and the second term is the difference between the empirical CDF of the scenario tree and the CDF of the data. The first constraint guarantees that the summation of the probabilities is one, the second constraint computes the average of the scenario tree, and the third constraint defines the higher order moments.

The cumulative distribution function is approximated from the data. In general, different models can be used, such as the logistic function, neural networks, decision trees, etc. We use symbolic regression to learn a model G. The symbolic regression task

is solved using `gplearn` (0.4.2) [29], which implements a genetic programming algorithm. The learned function is equal to:

$$G(a_s) = \frac{a_s^2}{a_s^2 - 0.035a_s + 0.044}. \tag{13}$$

The fourth constraint in Equation (12) defines the error e_s between the CDF from the data for α_s, $G(\alpha_s)$ and the ECDF from the scenario tree $\sum_{s'=1}^{s} \pi_{s'}$ (see [28] for a detailed description of the scenario generation problem).

The optimization problem in Equation (12) is a nonconvex nonlinear optimization problem. Although it can be solved with a global optimization solver, this can be computationally expensive. To reduce the computational time, we use a multi-start approach [30], implemented in Pyomo (6.4.4) [31], which solves multiple nonlinear optimization problems using IPOPT (3.11.1.0) [32] for different initial guesses. We use the high-confidence stopping rule, and all the other hyperparameters are set equal to their default values (see [30,31] for details on these hyperparameters). We generate ten scenarios for use in the ammonia supply chain transition case study. The CPU time for solving the scenario generation problem (Equation (12)) with the multistart approach is 3 min. The data for the different scenarios are presented in Figure 2 and Table 1.

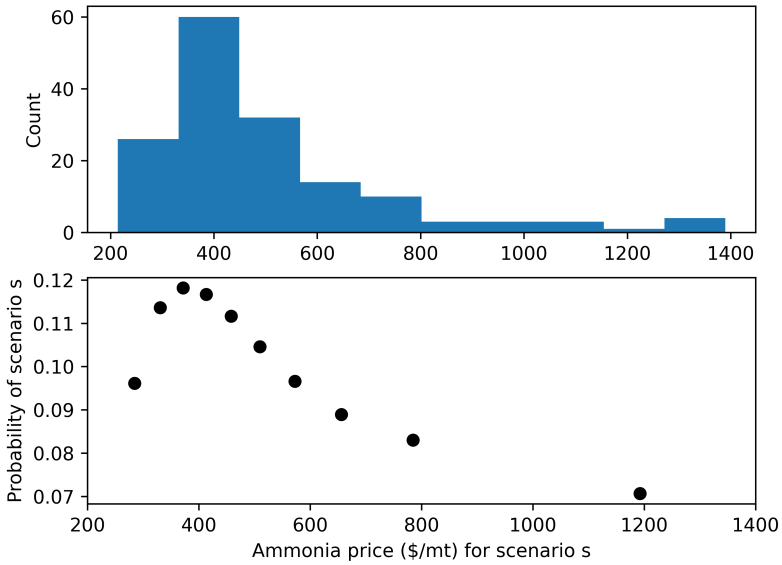

Figure 2. Information for the different generated 10 scenarios. The (**top**) is the histogram computed from the data, and the (**bottom**) is the ammonia price and probability for each scenario.

Table 1. Ten conventional ammonia price scenarios and their associated probability obtained from the scenario generation optimization problem.

Scenario Number	Ammonia Price ($/mt)	Probability
1	284.65	0.0961
2	330.60	0.1135
3	371.60	0.1181
4	413.16	0.1166
5	458.21	0.1116
6	509.82	0.1045
7	572.65	0.0966
8	655.88	0.0889
9	784.83	0.0830
10	1192.40	0.0706

4. Numerical Results

We solve deterministic and stochastic supply chain transition optimization models for the Minnesota case study. The deterministic model corresponds to a two-stage stochastic model using one scenario with a probability equal to one. We specifically solve the deterministic model for a nominal conventional ammonia price of 500 USD/mt, computed from the historical data presented in Figure 1. We consider two supply chain transition cases: one purely based on economics and one where the entire ammonia demand must be met with renewable production by 2032. All the optimization problems are solved using Gurobi (10.0.2.0) [33].

4.1. Economically Optimal Supply Chain Transition

4.1.1. Deterministic Case

The deterministic problem has 22,194 variables and 1,803 constraints and is solved in less than a second. The total net present cost is 2,978 million (MM) USD, and three new renewable ammonia sites with cumulative capacity equal to 297.69 mt are installed by the end of the horizon. This corresponds to only 35% of the ammonia demand being met with renewable production. All new facilities are installed in 2027, meaning that in-state production starts in 2029. These facilities are located in Southwest Minnesota, which has the highest wind potential at 52% annual average capacity factor. The new facilities in Lake Wilson and Chandler each require 250 MW of wind capacity and thus have the largest possible nameplate capacity. The nameplate capacity of the Wilmont facility is such that the total required electrolysis capacity across the three optimal sites is 575 MW, the maximum amount that can be procured in 2027.

4.1.2. Stochastic Case

The stochastic problem has 217,566 variables and 11,927 constraints and is solved in seven seconds. The total net present cost is 3,082 MM USD, and five new renewable ammonia sites with cumulative capacity equal to 540.17 mt are installed by the end of the horizon. This corresponds to 63.5% of the ammonia demand being met with in-state renewable production. Renewable production installed in 2027 has the same location and scale as in the deterministic case. Two additional facilities are installed in Southwest Minnesota in 2028, each with capacity that corresponds to 250 MW of wind. Evidently, economies of scale are important in the transition to in-state renewable ammonia production.

4.1.3. Comparison of the Deterministic and Stochastic Solution for the Economically Optimal Supply Chain Transition

Comparing the optimal supply chain transition decisions between the deterministic and stochastic case, the first observation is more renewable ammonia production capacity. Including scenarios with higher-than-average price of ammonia results in more in-state ammonia production and consequently fewer conventional ammonia purchases over the planning horizon compared to the deterministic case. From Figure 3, we observe that the amount of ammonia purchased from conventional resources between 2024 and 2029 is the same for the deterministic and stochastic cases since until 2027, the same investment decisions are made for both cases (see Tables 2 and 3). However, for the stochastic case, after 2030, less ammonia is purchased from conventional producers due to the investments made in 2028. This leads to lower conventional ammonia purchasing and transportation costs, along with higher capital and operating cost as shown in Figure 4. Overall, the net present cost for the stochastic case is 3.4% higher than the deterministic case.

Table 2. Installation year, location, and capacity for new renewable ammonia production in the deterministic case for the economically optimal supply chain transition. Annual average wind capacity factors for each selected candidate location are provided in parentheses to describe the wind potential.

Year	Location	Capacity (mt/y)	Wind (MW)	Electrolysis (MW)
2027	Lake Wilson (52%)	121.24	250	234
2027	Chandler (52%)	121.24	250	234
2027	Wilmont (52%)	55.21	114	107

Table 3. Installation year, location, and capacity for new renewable ammonia production in the two-stage stochastic case for the economically optimal supply chain transition. Annual average wind capacity factors for each selected candidate location are provided in parentheses to describe the wind potential.

Year	Location	Capacity (mt/y)	Wind (MW)	Electrolysis (MW)
2027	Lake Wilson (52%)	121.24	250	234
2027	Chandler (52%)	121.24	250	234
2027	Wilmont (52%)	55.21	114	107
2028	Luverne (52%)	121.24	250	234
2028	Worthington (52%)	121.24	250	234

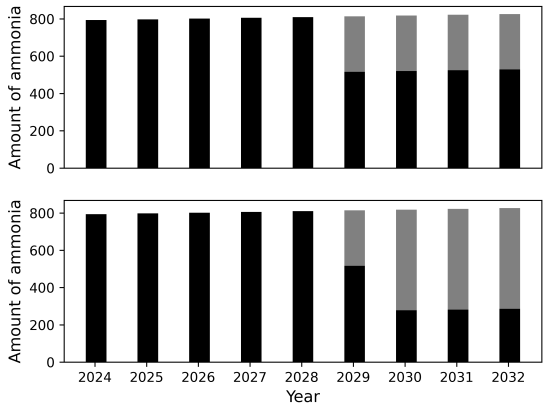

Figure 3. Amount of ammonia in each year sourced from conventional purchases (black bar) and in-state renewable ammonia production (gray bar) for the deterministic (**top**) and stochastic (**bottom**) cases for the economically optimal supply chain transition.

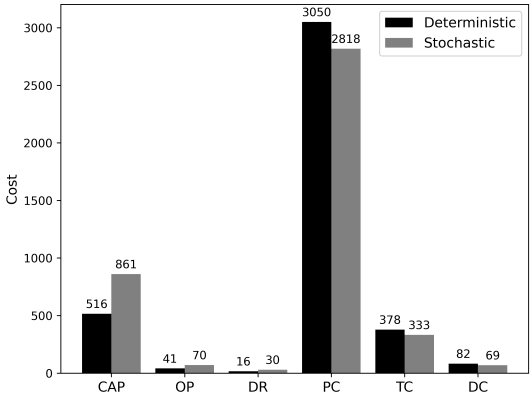

Figure 4. Cost contributions to optimal net present cost for the deterministic and stochastic cases for the economically optimal supply chain transition. The cost acronyms are defined as follows: CAP—renewable capital, OP—renewable operating, DR—renewable distribution, PC—conventional purchase, TC—conventional transportation to Minnesota, DC—conventional distribution.

We also compare the net present costs of the supply chain configurations obtained from the deterministic and stochastic cases. Specifically, for each optimal supply chain transition, we fix the capacity expansion decisions (binary variables related to the period an investment is made and the installed capacity) and compute the net present cost of the supply chain transition for different conventional ammonia prices. We perform these calculations for 100 values of ammonia price sampled uniformly between 214 USD/mt and 1,389 USD/mt and the results are presented in Figure 5. We observe that for prices of ammonia above 800 USD/mt, the net present cost of the supply chain obtained via stochastic programming is meaningfully lower than the cost of the deterministic design, whereas for low prices of ammonia (below 400 USD/mt), the opposite holds. This result can be attributed to the higher capacity installed in the stochastic case, which results in less reliance on the volatile conventional ammonia market.

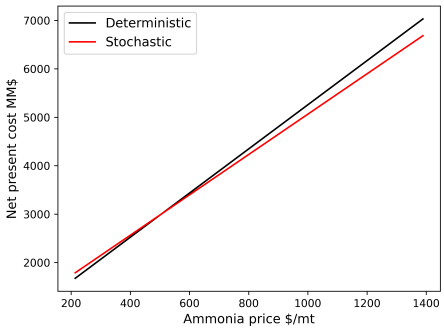

Figure 5. Net present cost for the deterministic and stochastic design as a function of the ammonia price for the economically optimal supply chain transition.

4.2. Optimal Supply Chain Transition to Full Renewable Production by 2032

We also aim to understand the economics and temporal profile of a full transition to in-state renewable ammonia production by the end of 2032. To this end, we include the following constraint in the formulation:

$$\sum_{p \in \mathcal{P}} \sum_{d \in \mathcal{D}} y_{pd|\mathcal{K}|s} = 0 \quad \forall s \in \mathcal{S}, \tag{14}$$

which enforces that no ammonia can be purchased from conventional producers in the year of the transition horizon.

4.2.1. Deterministic Case

We solve the deterministic problem for the nominal value of ammonia price equal to 500 USD/mt and obtain the optimal solution in less than a second. The total net present cost is 3,002 million USD, and eight renewable sites are installed (see Table 4).

Table 4. Installation year, location, and capacity for new renewable ammonia production in the deterministic case for fully renewable ammonia production. Annual average wind capacity factors for each selected candidate location are provided in parentheses to describe the wind potential.

Year	Location	Capacity (mt/y)	Wind (MW)	Electrolysis (MW)
2027	Lake Wilson (52%)	121.24	250	234
2027	Chandler (52%)	121.24	250	234
2027	Worthington (52%)	55.21	114	107
2027	Luverne (52%)	121.24	250	234
2028	Worthington (52%)	66.03	136	128
2028	Wilmont (52%)	110.42	228	213
2030	Blue Earth (47%)	116.13	250	235
2030	Winnebago (47%)	114.76	247	232

The first in-state renewable ammonia production starts in 2029, meaning that the demand is satisfied completely from conventional resources for the first five years of the transition. The first six facilities are located in Southwest Minnesota, which has the highest wind capacity factor (52%). In 2027 and 2028, the maximum amount of electrolysis is procured (575 MW); this results in smaller facilities installed in Worthington in both years. The last two facilities are installed in 2030 to guarantee that the ammonia demand in 2032 is fully met by renewable production. These two facilities are located in Southeast Minnesota, which also has a relatively high wind capacity factor (47%). Finally, we observe that in an attempt to achieve economies of scale, all installed facilities, except the two small ones in Worthington, use at least 225 MW of wind generation.

4.2.2. Stochastic Case

We obtain the solution to the stochastic problem in 28 s. The net present cost is 3100 MM USD, and the renewable sites installed are presented in Table 5.

Table 5. Installation year, location, and capacity for new renewable ammonia production in the two-stage stochastic case for fully renewable ammonia production. Annual average wind capacity factors for each selected candidate location are provided in parentheses to describe the wind potential.

Year	Location	Capacity (mt/y)	Wind (MW)	Electrolysis (MW)
2024	Lake Wilson (52%)	117.7	250	233
2027	Chandler (52%)	121.24	250	234
2027	Luverne (52%)	121.24	250	234
2027	Blue Earth (47%)	50.71	114	107
2028	Worthington (52%)	121.24	250	234
2028	Wilmont (52%)	121.24	250	234
2030	Blue Earth (47%)	63.13	136	128
2030	Winnebago (47%)	109.77	236	222

Eight new renewable facilities are installed as with the deterministic case. However, some installations occur earlier in the stochastic case, specifically as early as 2024 in Lake Wilson. This early investment allows market penetration of renewable ammonia by 2026, three years earlier than the deterministic case. We observe the same general trends pertaining to facility location and scale as in the deterministic case. Specifically, all facilities are located in Southwest and Southeast Minnesota to take advantage of the high wind potentials, and most facilities use more than 225 MW of co-located wind generation to achieve economies of scale.

4.2.3. Comparison of the Deterministic and Stochastic Solution for the Transition to Full Renewable Production

The total capacity installed in the deterministic and stochastic cases is the same, 826 mt. However, the individual costs are different. Specifically, the earlier introduction of in-state renewable ammonia production in the stochastic case leads to fewer conventional purchases over the planning horizon compared to the deterministic case (see Figure 6). This results in lower purchase, transportation, and distribution costs over the planning horizon (see Figure 7).

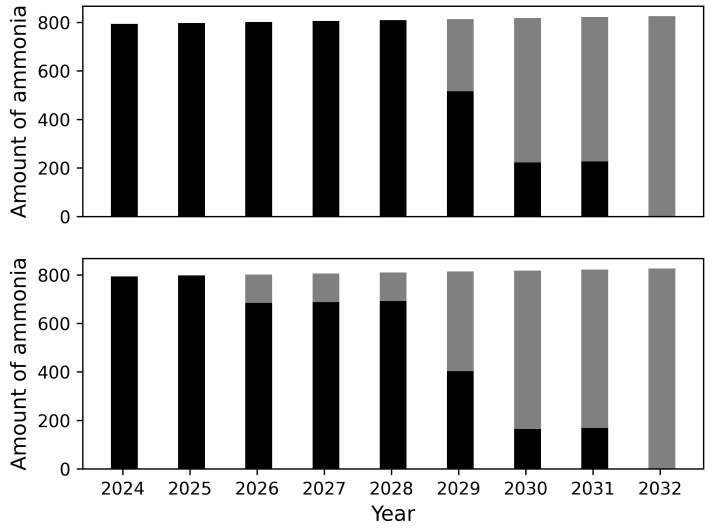

Figure 6. Amount of ammonia in each time period from conventional purchases (black bar) and in-state renewable ammonia production (gray bar) for the deterministic (**top**) and stochastic (**bottom**) cases for fully renewable ammonia production.

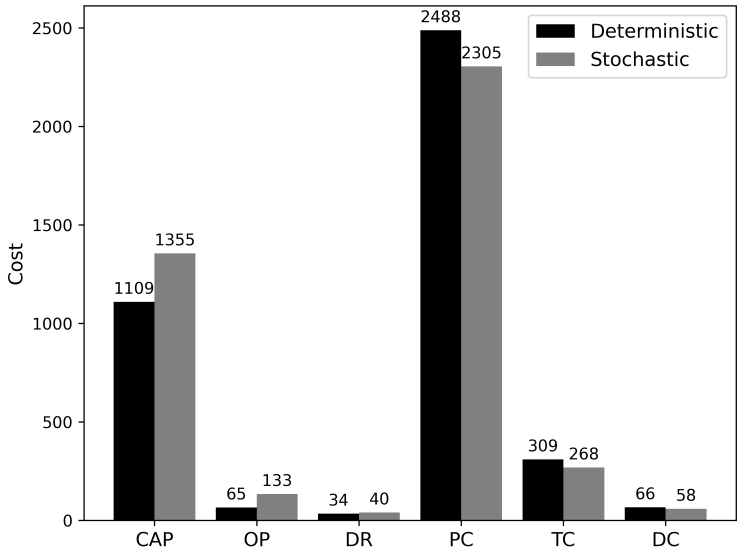

Figure 7. Cost contributions to optimal net present cost for the deterministic and stochastic cases for fully renewable ammonia production. The cost acronyms are defined as follows: CAP—renewable capital, OP—renewable operating, DR—renewable distribution, PC—conventional purchase, TC—conventional transportation to Minnesota, DC—conventional distribution.

On the other hand, the capital investment is higher for the stochastic design because the first renewable production is installed earlier in the planning horizon when the constituent technologies are more expensive. The operating cost is also higher in the stochastic case both for the above-described reason and because more renewable ammonia is produced over the transition horizon (e.g., more renewable energy is purchased). Overall, the net present cost for the supply chain transition is 3.2% (98 MM USD) higher in the stochastic case.

Finally, we compare the net levelized costs obtained from the deterministic and stochastic supply chain transitions. Similar to Section 4.1.3, we fix the investment decisions (time of investment and capacity) and discretize the ammonia price in 100 uniform points between 214 USD/mt and 1389 USD/mt. The net present cost for the two designs as a function of ammonia price is presented in Figure 8. From these results, we observe that for conventional ammonia prices above 700 USD/mt, the net levelized cost of the design obtained in the stochastic case is lower than that in the deterministic case since less ammonia is purchased

from conventional resources. The benefit of local renewable ammonia production with respect to providing price stability in the face of the volatile conventional ammonia market is even more pronounced than in the purely economic case.

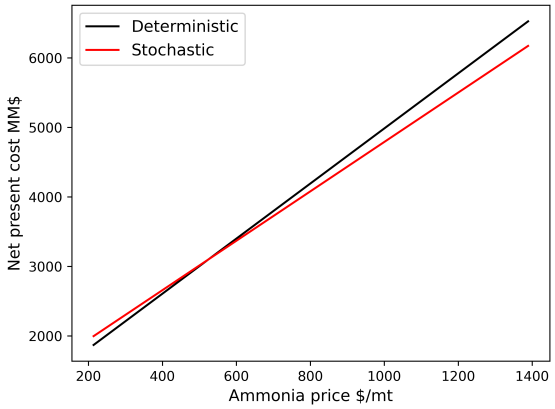

Figure 8. Levelized cost for the deterministic and stochastic design as a function of ammonia price for complete renewable ammonia.

5. Conclusions

In this work, we considered the effect of price uncertainty on the transition of ammonia supply chain networks from fossil-derived ammonia imported from out-of-state conventional producers to in-state renewable ammonia production. We employed a two-stage stochastic programming approach to determine the optimal investment decisions over a transition horizon such that the ammonia demand is satisfied while the net present cost is minimized.

First, we considered the economically optimal supply chain transition. The results show that accounting for uncertainty leads to the installation of higher renewable production capacity compared to the deterministic case. This results in a reduction in ammonia purchases from conventional producers and thus lower purchasing costs. We also considered the effect of price uncertainty on the optimal transition to a completely renewable ammonia supply chain network. In this case, investments are made earlier in the planning horizon compared to a deterministic supply chain transition model, which again reduces conventional ammonia purchase costs. Overall, the results show that in-state renewable ammonia production can provide stable ammonia costs and act as a hedge against the possibility of high conventional prices and, more generally, the volatility of the existing ammonia market.

In this work, we assumed that the price of ammonia is constant across the entire planning horizon and thus followed a two-stage stochastic programming approach. However, in practice, ammonia prices can evolve differently across multi-year trajectories due to a variety of market factors. Future work will consider a multi-stage stochastic programming approach. However, this will entail large optimization problems, which might require tailored decomposition-based optimization algorithms [34,35]. Additionally, future work will incorporate other sources of exogenous and endogenous uncertainty such as change in electrolysis costs, which are expected to decrease due to wider adoption as well as research and development.

Author Contributions: Conceptualization, I.M., M.J.P. and P.D.; methodology, I.M., M.J.P. and P.D.; software, I.M.; validation, I.M., M.J.P. and P.D.; formal analysis, I.M., M.J.P. and P.D.; investigation, I.M., and M.J.P.; data curation, I.M. and M.J.P.; writing—original draft preparation, I.M. and M.J.P.; writing—review and editing, I.M., M.J.P. and P.D.; visualization, I.M., M.J.P. and P.D.; supervision, P.D.; project administration, P.D.; funding acquisition, P.D. All authors have read and agreed to the published version of the manuscript.

Funding: The work was funded in part by NSF CBET (award number 2313289) and the Advanced Research Projects Agency-Energy (ARPA-E), U.S. Department of Energy, under Award Number DE-AR0001479. The views and opinions of authors expressed herein do not necessarily state or reflect those of the United States Government or any agency thereof.

Data Availability Statement: Data will be made available upon request.

Conflicts of Interest: The authors declare no conflicts of interest. The funders had no role in the design of the study; in the collection, analyses, or interpretation of data; in the writing of the manuscript; or in the decision to publish the results.

References

1. Smith, C.; Hill, A.K.; Torrente-Murciano, L. Current and future role of Haber–Bosch ammonia in a carbon-free energy landscape. *Energy Environ. Sci.* **2020**, *13*, 331–344.
2. Rouwenhorst, K.H.; Travis, A.S.; Lefferts, L. 1921–2021: A Century of renewable ammonia synthesis. *Sustain. Chem.* **2022**, *3*, 149–171.
3. Royal Society. *Ammonia: Zero-carbon Fertiliser, Fuel and Energy Store: Policy Briefing*; Royal Society: London, UK, 2020.
4. Schiffer, Z.J.; Manthiram, K. Electrification and decarbonization of the chemical industry. *Joule* **2017**, *1*, 10–14.
5. Allman, A.; Daoutidis, P.; Tiffany, D.; Kelley, S. A framework for ammonia supply chain optimization incorporating conventional and renewable generation. *AIChE J.* **2017**, *63*, 4390–4402.
6. Palys, M.J.; Allman, A.; Daoutidis, P. Exploring the benefits of modular renewable-powered ammonia production: A supply chain optimization study. *Ind. Eng. Chem. Res.* **2018**, *58*, 5898–5908.
7. Osorio-Tejada, J.; Tran, N.N.; Hessel, V. Techno-environmental assessment of small-scale Haber-Bosch and plasma-assisted ammonia supply chains. *Sci. Total Environ.* **2022**, *826*, 154162.
8. Palys, M.J.; Daoutidis, P. Power-to-X: A review and perspective. *Comput. Chem. Eng.* **2022**, *165*, 107948.
9. Wiskich, A.; Rapson, T. Economics of Emerging Ammonia Fertilizer Production Methods–a Role for On-Farm Synthesis? *ChemSusChem* **2023**, *16*, e202300565.
10. U.S. Environmental Protection Agency. *Commercial Fertilizer Purchased*; U.S. Environmental Protection Agency: Washington, DC, USA, 2023.
11. Armijo, J.; Philibert, C. Flexible production of green hydrogen and ammonia from variable solar and wind energy: Case study of Chile and Argentina. *Int. J. Hydrogen Energy* **2020**, *45*, 1541–1558.
12. Fasihi, M.; Weiss, R.; Savolainen, J.; Breyer, C. Global potential of green ammonia based on hybrid PV-wind power plants. *Appl. Energy* **2021**, *294*, 116170.
13. Etienne, X.L.; Trujillo-Barrera, A.; Wiggins, S. Price and volatility transmissions between natural gas, fertilizer, and corn markets. *Agric. Financ. Rev.* **2016**, *76*, 151–171.
14. Isella, A.; Lista, A.; Colombo, G.; Ostuni, R.; Manca, D. Gray and hybrid green ammonia price sensitivity to market fluctuations: The Russia-Ukraine war case. In *Computer Aided Chemical Engineering*; Elsevier: Amsterdam, The Netherlands, 2023; Volume 52, pp. 2285–2290.
15. Ahmed, S. *Strategic Planning under Uncertainty: Stochastic Integer Programming Approaches*; University of Illinois at Urbana-Champaign: Urbana, IL, USA, 2000.
16. Palys, M.J.; Daoutidis, P. Optimizing renewable ammonia production for a sustainable fertilizer supply chain transition. *ChemSusChem* **2023**, *16*, e202300563.
17. Grossmann, I.E.; Apap, R.M.; Calfa, B.A.; García-Herreros, P.; Zhang, Q. Recent advances in mathematical programming techniques for the optimization of process systems under uncertainty. *Comput. Chem. Eng.* **2016**, *91*, 3–14.
18. Gupta, A.; Maranas, C.D. Managing demand uncertainty in supply chain planning. *Comput. Chem. Eng.* **2003**, *27*, 1219–1227.
19. Goel, V.; Grossmann, I.E. A class of stochastic programs with decision dependent uncertainty. *Math. Program.* **2006**, *108*, 355–394.
20. Rathi, T.; Zhang, Q. Capacity planning with uncertain endogenous technology learning. *Comput. Chem. Eng.* **2022**, *164*, 107868.
21. Marufuzzaman, M.; Eksioglu, S.D.; Huang, Y.E. Two-stage stochastic programming supply chain model for biodiesel production via wastewater treatment. *Comput. Oper. Res.* **2014**, *49*, 1–17.
22. Chen, C.W.; Fan, Y. Bioethanol supply chain system planning under supply and demand uncertainties. *Transp. Res. Part E: Logist. Transp. Rev.* **2012**, *48*, 150–164.
23. Dal-Mas, M.; Giarola, S.; Zamboni, A.; Bezzo, F. Strategic design and investment capacity planning of the ethanol supply chain under price uncertainty. *Biomass Bioenergy* **2011**, *35*, 2059–2071.
24. Zhou, X.; Zhang, H.; Qiu, R.; Lv, M.; Xiang, C.; Long, Y.; Liang, Y. A two-stage stochastic programming model for the optimal planning of a coal-to-liquids supply chain under demand uncertainty. *J. Clean. Prod.* **2019**, *228*, 10–28.
25. The World Bank. *Commodity Markets*; The World Bank: Washington, DC, USA, 2023.
26. Govindan, K.; Fattahi, M.; Keyvanshokooh, E. Supply chain network design under uncertainty: A comprehensive review and future research directions. *Eur. J. Oper. Res.* **2017**, *263*, 108–141.
27. 17th U. S. Congress. Inflation Reduction Act of 2022, H.R.5376 2022. Available online: https://www.congress.gov/bill/117th-congress/house-bill/5376 (accessed on 1 March 2023).

28. Calfa, B.A.; Agarwal, A.; Grossmann, I.E.; Wassick, J.M. Data-driven multi-stage scenario tree generation via statistical property and distribution matching. *Comput. Chem. Eng.* **2014**, *68*, 7–23.
29. Stephens, T. gplearn: Genetic Programming in Python, with a Scikit-Learn Inspired Api. 2015. Available online: https://gplearn.readthedocs.io/en/stable/ (accessed on 1 December 2023).
30. Dick, T.; Wong, E.; Dann, C. *How Many Random Restarts Are Enough*; Technical Report; Carnegie Mellon University: Pittsburgh, PA, USA, 2014.
31. Hart, W.E.; Watson, J.P.; Woodruff, D.L. Pyomo: Modeling and solving mathematical programs in Python. *Math. Program. Comput.* **2011**, *3*, 219–260.
32. Wächter, A.; Biegler, L.T. On the implementation of an interior-point filter line-search algorithm for large-scale nonlinear programming. *Math. Program.* **2006**, *106*, 25–57.
33. Gurobi Optimization, LLC. Gurobi Optimizer Reference Manual; Gurobi Optimization, LLC: Beaverton, OR, USA, 2023.
34. Mitrai, I.; Tang, W.; Daoutidis, P. Stochastic blockmodeling for learning the structure of optimization problems. *AIChE J.* **2022**, *68*, e17415.
35. Allen, R.C.; Iseri, F.; Demirhan, C.D.; Pappas, I.; Pistikopoulos, E.N. Improvements for decomposition based methods utilized in the development of multi-scale energy systems. *Comput. Chem. Eng.* **2023**, *170*, 108135.